

Influencing factors on false positive rates when classifying tumor cell line response to drug treatment

Priyanka Vasanthakumari¹, Thomas Brettin¹, Yitan Zhu¹, Hyunseung Yoo¹, Maulik Shukla¹, Alexander Partin¹, Fangfang Xia¹, Oleksandr Narykov¹, and Rick L. Stevens^{1,2}

1 Computing, Environment and Life Sciences, Argonne National Laboratory, Lemont, IL

2 Department of Computer Science, The University of Chicago, Chicago, IL

Abstract

Informed selection of drug candidates for laboratory experimentation provides an efficient means of identifying suitable anti-cancer treatments. The advancement of artificial intelligence has led to the development of computational models to predict cancer cell line response to drug treatment. It is important to analyze the false positive rate (FPR) of the models, to increase the number of effective treatments identified and to minimize unnecessary laboratory experimentation. Such analysis will also aid in identifying drugs or cancer types that require more data collection to improve model predictions. This work uses an attention based neural network classification model to identify responsive/non-responsive drug treatments across multiple types of cancer cell lines. Two data filtering techniques have been applied to generate 10 data subsets, including removing samples for which dose response curves are poorly fitted and removing samples whose area under the dose response curve (AUC) values are marginal around 0.5 from the training set. One hundred trials of 10-fold cross-validation analysis is performed to test the model prediction performance on all the data subsets and the subset with the best model prediction performance is selected for further analysis. Several error analysis metrics such as the false positive rate (FPR), and the prediction uncertainty are evaluated, and the results are summarized by cancer type and drug mechanism of action (MoA) category. The FPR of cancer type spans between 0.262 and 0.5189, while that of drug MoA category spans almost the full range of [0, 1]. This study identifies cancer types and drug MoAs with high FPRs. Additional drug screening data of these cancer and drug categories may improve response modeling. Our results also demonstrate that the two data filtering approaches help improve the drug response prediction performance.

Keywords: Anti-cancer drug response prediction, data filtering, false positive rate, error analysis

1. Introduction

Screening drugs to target specific diseases in the laboratory requires an informed selection of drug candidates. Recent advances in drug discovery such as the high throughput screening facilitates testing a huge number of drugs at a much faster rate than traditional techniques. Cancer is a highly heterogenous disease and precision medicine allows physicians to offer personalized treatment options to patients based on their individual cancer types. Computational methods [1–13] for anti-cancer drug response prediction aids in identifying suitable drugs for specific cancer types based on comprehensive genomic analysis. It is important to analyze the false positive rates (FPR) while using such computational drug response models to minimize the number of experimentation as well as to improve the model performance by collecting more data for experiments with poor FPR.

Our approach in this study is to identify candidate drugs for laboratory screening using a deep neural network classifier (DNN) that predicts whether a cell line will respond to the drug treatment. Several studies[14–17] have generated and reported dose response curves constructed by measuring the growth response of cancer cell lines exposed to drug treatments under study. The dataset used in this work is constructed by including 21 cancer types that have the largest numbers of cell lines with RNA-Seq and drug response data available in a combined set of five drug screening studies. The cell lines are represented by gene expression profiles and the drugs are represented by molecular descriptors. An attention based neural network classification model is used to predict responsive vs. non-responsive treatments. The response labels used for training our classifier are derived by computing the normalized area under the dose response curve (AUC) and assigning a responder or non-responder label to the sample if the AUC is greater or less than some threshold.

This study investigates false positives relative to true positives using the DNN classifier through 100 trials of 10-fold cross-validation. Two data filtering techniques have been applied, including removing samples for which dose response curves are poorly fitted and removing samples whose AUC values are marginal around 0.5 from the training set. This analysis examines the effect of the choice of the threshold that is applied on AUC values for calling response vs. nonresponse, and the selection of samples based on the goodness of fit when computing the dose response curve. Our analysis results show both filtering approaches help improve the model prediction performance. The FPRs of 21 cancer types and 96 different drug mechanism of action (MoA) categories are summarized for the best performing models. The major contributions of this work are: 1) implementing data filtering approaches to improve drug response prediction performance, and 2) identifying cancer types and drug MoAs with high FPRs. Generating more data for cancer types and drug MoA categories with high FPRs, can potentially improve the model performance for predicting responses of these cancer types and drug MoA categories.

2. Methods

2.1. Data and data splitting strategy

The dataset was constructed by including top 21 cancer types having the greatest number of cell lines with the RNA-Seq and drug response data available in the combined set of CTRP[17], CCLE[14], gCSI[15], NCI-60[18] and GDSC[16] studies. The drug response dataset from the top 21 cancer types consists of 1895 cancer cell lines and 1681 anti-cancer drugs. A sample in the

dataset represents a cell line treated with a single drug. The cell lines are represented by gene expression values for 942 benchmark genes from the LINCS[19] study and the drugs are represented by 5270 molecular drug descriptors computed using the Dragon7 software[20].

The AUC value from the dose response curve is calculated and used for determining the classes for the classification task. The experiment samples are categorized into the non-responders ($AUC \geq 0.5$) and responders ($AUC < 0.5$) and encoded to 0 and 1, respectively. Because drug response data were merged from multiple studies, several experiments (i.e. pairs of cell lines and drugs) had contradicting responses. After removing samples with contradicting responses and duplicated samples, the dataset consisted of 339,896 samples, and the response categories were highly skewed: 95% non-responders, 5% responders. The data is highly unbalanced, as would be expected. There are many more cases when the cancer cells do not respond to the drug treatment.

After building the top21 dataset, we recognized that some experiments did not have a dose response curve fitted well (28% have R-squared fit score < 0.5). Hence the samples with poor R-squared fit scores could confuse model training. Similarly, because of inherent error in fitting the dose-response curve, samples with an AUC close to 0.5 might not be trustworthy. To understand the impacts of samples with a poor dose-response curve fitting and samples near the AUC boundary, we developed three filtering levels (0.0, 0.5, and 0.9) on R-squared fit score and two gap conditions, removing samples around the boundary (AUC between 0.4 and 0.6 - gap1) or samples above the boundary (between 0.5 and 0.7 - gap2). This approach resulted in 10 datasets, each subjected to 100 10-fold cross-validation trials. Table 1 shows the 10 different datasets, their descriptions and the numbers of drugs and cell lines in data.

100 10-fold cross-validation experiments were conducted on each dataset. Each dataset was split into training, validation, and test sets 100 times, with each split being a random 80% training, 10% validation and 10% testing. The samples column in Table 1 shows the number of samples in training, validation, and testing sets. 100 models were trained using the 100 splits of data. The model was trained on the training set and predictions were generated on the testing set for every data split.

2.2 Model architecture

This work uses a deep neural network model with attention mechanism. The code base and implementation details of the model (named as ‘Attn’) can be found in the Benchmarks [repository](#) (of the Exa-scale computing project (ECP) application Cancer Distributed Learning Environment (CANDLE)[21]). It utilizes the CANDLE Benchmark infrastructure for quick setup and hyperparameter optimization using the CANDLE Supervisor framework. The Attn model is trained on gene expressions of cancer cell lines and molecular descriptors of drugs to classify the treatment effect as either response or non-response. The trained model is neither cancer nor drug specific.

The model is compiled into 9 layers, consisting of 7 hidden, input and output layers. Input layer has 6212 neurons, the output layer has a single neuron. The 8 hidden layers have 1000, 500, 250, 125, 60, 30, 2. The softmax activation function is used for the first and last hidden layer, while the rest of the layers are set to ReLU. A dropout rate of 0.2 is used. The loss function is set to categorical cross-entropy, which is used for single label prediction, and the SGD optimizer is used.

Table 1. Summary of datasets used for 100 trials of 10-fold cross-validation. Each dataset consists of precomputed randomized training, validation, and testing sets. The number of samples in the training, validation, and testing sets, along with the numbers of drugs and cell lines are shown. The table also shows the MCC values obtained after the 100 trials of 10-fold cross-validation were done on each dataset.

Dataset	# Samples in: Training Validation Testing	Drugs : Cell lines	MCC	Description
top21_baseline	271,915 33,989 33,989	1017:1204	0.61912237	Splits of top_21.res_bin.cf_rnaseq.dd_dragon7.labeled.scaled.debug.parquet
top21_r.0_baseline	269,811 33,726 33,726	1018:1204	0.61809175	No AUC gap condition. Samples with R-squared fit value less than 0.0 are removed from training.
top21_r.0_gap1	255,685 33,726 33,726	1018:1204	0.62442323	Removes samples from training with the value of the AUC between 0.4 and 0.6, and R-squared fit value less than 0.0
top21_r.0_gap2	245,117 33,726 33,726	1018:1204	0.58580431	Removes samples from training with the value of the AUC between 0.5 and 0.7, and R-squared fit value less than 0.0
top21_r.5_baseline	201,895 25,236 25,237	991:1204	0.61901118	No AUC gap condition. Samples with R-squared fit value less than 0.5 are removed from training.
top21_r.5_gap1	187,973 25,236 25,237	991:1204	0.62321287	Removes samples from training with the value of the AUC between 0.4 and 0.6, and R-squared fit value less than 0.5
top21_r.5_gap2	177,567 25,236 25,237	991:1204	0.58677235	Removes samples from training with the value of the AUC between 0.5 and 0.7, and R-squared fit value less than 0.5
top21_r.9_baseline	144,807 18,101 18,101	941:1204	0.62977115	No AUC gap condition. Samples with R-squared fit value less than 0.9 are removed from training.
top21_r.9_gap1	133,307 18,101 18,101	941:1204	0.63474431	Removes samples from training with the value of the AUC between 0.4 and 0.6, and R-squared fit value less than 0.9
top21_r.9_gap2	124,565 18,101 18,101	941:1204	0.59180333	Removes samples from training with the value of the AUC between 0.5 and 0.7, and R-squared fit value less than 0.9

2.3 False positive rate analysis

The deep neural network model is trained on each of the 10 datasets described in Table 1. 100 trials of 10-fold cross-validation analysis is performed using each dataset. The performance of the model is analyzed using Mathew’s correlation coefficient (MCC). A high value of MCC metric can be obtained only if the model correctly classifies high percentages of both response and nonresponse samples, irrespective of class imbalances. Therefore, due to the high-class imbalance between responders and non-responders, MCC will be a good metric to assess the model classification performance. The effect of the two filtering approaches in building the 10 datasets

can be evaluated using the MCC scores. The dataset with the best MCC score is then chosen for further analysis.

The prediction outcomes from the selected dataset are categorized into true positives (TP), true negatives (TN), false positives (FP), and false negatives (FN) by comparing with the ground truth response values. The total numbers of TP, TN, FP, and FN are counted for each cancer type and each drug MoA category separately across all the 100 trials of 10-fold cross-validation. The following evaluation metrics are computed.

$$\text{False positive rate, } FPR = \frac{FP}{(FP+TP)} \quad (1)$$

$$\text{False negative rate, } FNR = \frac{FN}{(FN+TN)} \quad (2)$$

$$\text{Total false rate, } TFR = \frac{(FP+FN)}{(FP+TP+FN+TN)} \quad (3)$$

Because each pair of cell line and drug has been predicted multiple times in the cross-validation analysis, we can also calculate the uncertainty of the prediction using the following equation.

$$\text{Uncertainty} = 1 - \frac{\text{abs}(TP+FP-TN-FN)}{TP+FP+TN+FN} \quad (4)$$

where $\text{abs}(\bullet)$ calculates the absolute value of input. The uncertainty measure focuses on the variation of prediction outcome through cross-validation rather than its accuracy. Average uncertainty is first calculated for each cancer cell line, and then it is further averaged across the multiple cell lines of a cancer type. Similarly, average uncertainty is first calculated for each drug and then further averaged across all drugs in a MoA category.

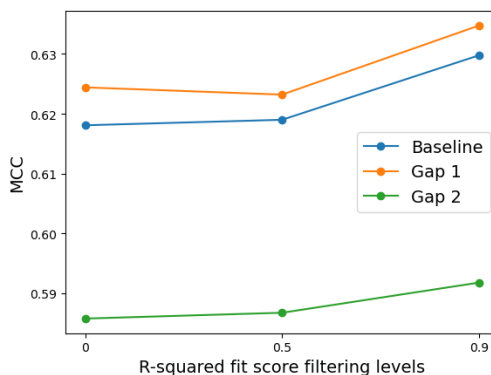


Figure 1 The variation in MCC with different data filtering approaches and thresholds.

3. Results

The MCC column in Table 1 shows the MCC scores obtained when training and evaluating the models on the 10 different datasets. Figure 1 shows the variation in MCC with the three filtering levels on the fitting score of dose response curve, for the three AUC gap conditions, i.e. baseline, gap1 and gap2. The best score is obtained when the dataset is generated using AUC gap1 condition and R-squared fit threshold of 0.9. Therefore, the analysis result of top21_r.9_gap1 dataset is chosen for further analysis. It can also be seen that the models trained on datasets filtered using AUC gap2 condition have much lower performances than the models trained on datasets using baseline or gap1 condition. Another major observation is that filtering using R-squared of 0.9 on

dose response curve fitting gives a prediction performance higher than filtering using R-squared of 0 and 0.5 with AUC gap condition unchanged.

The prediction results from the 100 trials of 10-fold cross-validation for models trained on top21_r.9_gap1 dataset are then analyzed. The TP, TN, FP, and FN counted for each cancer type and each drug MoA category are shown in Table 2 and Table 3, respectively. Both Table 2 and Table 3 are sorted according to the false positive rate. Only cancer types with at least 10 cell lines are shown in Table 2. Table 3 includes drug MoA categories with at least one positive sample, i.e. $TP + FN > 0$. Drug MoA categories without any positive sample, i.e., $TP = FN = 0$, are not shown in Table 3, because they may indicate “dead” MoA spaces without effective anti-cancer compounds. Average uncertainty for cancer types is shown in Table 2 and that of drug MoA category is shown in Table 3.

Reducing the FPR of predictions is important for improving the cost-efficiency of drug screening practice. A lower FPR leads to more validated effective treatments with the same number of experiments, since usually only experiments predicted to be responsive will be conducted. To reduce the FPR of prediction models, a reasonable strategy is to generate more data of cancer types and drug MoA categories with high FPRs, which are expected to improve the models for predicting responses of these cancer types and MoA categories. As shown in Table 2, the FPR of cancer type ranges from 0.262 to 0.5189. A weighted scheme can be applied to select cancer models from different cancer types for experiments, with the number of cancer models in each cancer type reversely proportional to its FPR. The prediction uncertainties of all cancer types are smaller than 0.05, which are not particularly useful for guiding experiment design. The FPR of drug MoA category spans almost the whole range of [0, 1]. For drug selection, MoA categories with high FPRs can be prioritized. On top of this selection criterion, we can further prioritize MoA categories which also have relatively high FNRs (e.g. > 0.1). Also, there are 12 MoA categories with a prediction uncertainty > 0.1 , which can also be prioritized for drug selection.

Table 2 Summary of prediction error and uncertainty by cancer type

Cancer Type	# TN	# TP	# FN	# FP	FNR	FPR	TFR	Uncertainty
Kidney Renal Clear Cell Carcinoma	65967	890	609	960	0.0091	0.5189	0.0229	0.0233
Ovarian Serous Cystadenocarcinoma	68210	1450	654	1322	0.0095	0.4769	0.0276	0.0276
Colon Adenocarcinoma	123019	3245	1563	2958	0.0125	0.4769	0.0346	0.0254
Breast Invasive Carcinoma	99705	3103	1327	2349	0.0131	0.4309	0.0345	0.0260
Liver Hepatocellular Carcinoma	45451	1273	659	953	0.0143	0.4281	0.0333	0.0233
Lung Squamous Cell Carcinoma	48626	1297	519	962	0.0106	0.4259	0.0288	0.0229
Lung Non-Small Cell Carcinoma	63813	2035	881	1505	0.0136	0.4251	0.0350	0.0207
Lung Adenocarcinoma	148251	4327	1994	3040	0.0133	0.4127	0.0319	0.0276
Lung Small Cell Carcinoma	79381	3361	1670	2249	0.0206	0.4009	0.0452	0.0294
Skin Cutaneous Melanoma	141321	3761	1573	2434	0.0110	0.3929	0.0269	0.0266
Glioblastoma Multiforme	60407	1966	800	1252	0.0131	0.3891	0.0319	0.0281
Stomach Adenocarcinoma	48636	1766	1029	1075	0.0207	0.3784	0.0401	0.0283
Uterine Corpus Endometrial Carcinoma	55856	1971	702	1174	0.0124	0.3733	0.0314	0.0232
Esophageal Carcinoma	58388	2282	854	1341	0.0144	0.3701	0.0349	0.0203
Ovary - other	42399	1187	442	675	0.0103	0.3625	0.0250	0.0201
Pancreatic Adenocarcinoma	57445	2049	737	1131	0.0127	0.3557	0.0304	0.0255
Head and Neck Squamous Cell Carcinoma	61522	2143	849	1162	0.0136	0.3516	0.0306	0.0182
Acute Myeloid Leukemia	49490	3616	1943	1657	0.0378	0.3142	0.0635	0.0444
Lymphoid Leukemia	137659	9521	4486	3887	0.0316	0.2899	0.0538	0.0441
Lymphoid Neoplasm Diffuse Large B-cell Lymphoma	56624	4820	2272	1757	0.0386	0.2671	0.0615	0.0436
Sarcoma	82321	4029	1695	1430	0.0202	0.2620	0.0349	0.0243

Table 3 Summary of prediction error and uncertainty by drug MoA category

MoA Category	# TN	# TP	# FN	# FP	Uncertainty	FNR	FPR	TFR	#TP + #FN
AKT Inhibitor	11976	0	63	3	0.0333	0.0052	1.0000	0.0055	63
ATR Kinase Inhibitor	2415	0	5	2	0.0008	0.0021	1.0000	0.0029	5
Bromodomain Inhibitor	18015	0	78	1	0.0007	0.0043	1.0000	0.0044	78
Bruton's Tyrosine Kinase (BTK) Inhibitor	5948	0	22	4	0.0036	0.0037	1.0000	0.0044	22
FGFR Inhibitor	18042	0	14	5	0.0004	0.0008	1.0000	0.0011	14
Hepatocyte Growth Factor Receptor Inhibitor	3114	0	9	1	0.0001	0.0029	1.0000	0.0032	9
JNK Inhibitor	11737	0	19	1	0.0002	0.0016	1.0000	0.0017	19
Leucine Rich Repeat Kinase Inhibitor	4957	0	7	26	0.0231	0.0014	1.0000	0.0066	7
Like (NRF2) Activator	3431	0	21	6	0.0034	0.0061	1.0000	0.0078	21
LXR Agonist	1409	0	13	1	0.0019	0.0091	1.0000	0.0098	13
MDM Inhibitor	16860	0	109	5	0.0062	0.0064	1.0000	0.0067	109
NEDD Activating Enzyme Inhibitor	5103	0	83	1	0.0005	0.0160	1.0000	0.0162	83
Nuclear Factor Erythroid Derived	3431	0	21	6	0.0034	0.0061	1.0000	0.0078	21
PARP Inhibitor	10715	0	98	39	0.0153	0.0091	1.0000	0.0126	98
Pyruvate Dehydrogenase Kinase Inhibitor	6280	0	20	10	0.0023	0.0032	1.0000	0.0048	20
RAF Inhibitor	24327	0	111	46	0.0059	0.0045	1.0000	0.0064	111
RET Tyrosine Kinase Inhibitor	23446	0	60	7	0.0004	0.0026	1.0000	0.0028	60
Retinoid Receptor Agonist	13625	0	18	2	0.0004	0.0013	1.0000	0.0015	18
Sphingolipid Biosynthesis Inhibitor	47	0	10	1	0.0357	0.1754	1.0000	0.1895	10
XIAP Inhibitor	4912	1	73	27	0.0091	0.0146	0.9643	0.0199	74
DNA Synthesis Inhibitor	13777	24	398	462	0.0609	0.0281	0.9506	0.0587	422
DNA Alkylating Agent	12541	23	296	380	0.0616	0.0231	0.9429	0.0511	319
ALK Tyrosine Kinase Receptor Inhibitor	12849	4	98	55	0.0566	0.0076	0.9322	0.0118	102
DNA Methyltransferase Inhibitor	8398	17	119	99	0.0174	0.0140	0.8534	0.0253	136
VEGFR Inhibitor	71888	2	193	9	0.0002	0.0027	0.8182	0.0028	195
Glucocorticoid Receptor Agonist	181	6	36	25	0.2590	0.1659	0.8065	0.2457	42
MCL1 Inhibitor	8305	7	76	22	0.0043	0.0091	0.7586	0.0117	83
Ephrin Inhibitor	5845	14	300	37	0.0288	0.0488	0.7255	0.0544	314
CHK Inhibitor	7243	37	247	86	0.0099	0.0330	0.6992	0.0437	284
KIT Inhibitor	46879	16	391	36	0.0033	0.0083	0.6923	0.0090	407
Cell Cycle Inhibitor	6604	56	342	121	0.0383	0.0492	0.6836	0.0650	398
Tyrosine Kinase Inhibitor	8519	14	287	29	0.0111	0.0326	0.6744	0.0357	301
IGF-1 Inhibitor	16736	13	153	24	0.0017	0.0091	0.6486	0.0105	166
MEK Inhibitor	15268	778	601	1421	0.1051	0.0379	0.6462	0.1119	1379
ATP Synthase Inhibitor	198	248	39	405	0.4282	0.1646	0.6202	0.4986	287
Growth Factor Receptor Inhibitor	2817	32	205	49	0.0194	0.0678	0.6049	0.0819	237
Protein Kinase C Inhibitor	41	81	23	120	0.4564	0.3594	0.5970	0.5387	104
BCL Inhibitor	23585	158	976	220	0.0326	0.0397	0.5820	0.0480	1134
JAK Inhibitor	26760	68	615	93	0.0095	0.0225	0.5776	0.0257	683
PDGFR Tyrosine Kinase Receptor Inhibitor	55829	50	475	62	0.0036	0.0084	0.5536	0.0095	525
Exportin Antagonist	6156	174	261	210	0.0342	0.0407	0.5469	0.0693	435
BCR-ABL Kinase Inhibitor	18167	57	432	68	0.0104	0.0232	0.5440	0.0267	489
FLT3 Inhibitor	39793	81	454	93	0.0066	0.0113	0.5345	0.0135	535
Inhibitor Of STAT3/JAK2 Signaling	3805	29	344	33	0.0285	0.0829	0.5323	0.0895	373
Lipocortin Synthesis Stimulant	3805	29	344	33	0.0285	0.0829	0.5323	0.0895	373
STAT Inhibitor	8382	29	344	33	0.0057	0.0394	0.5323	0.0429	373

MTOR Inhibitor	31029	1689	1659	1816	0.0520	0.0508	0.5181	0.0960	3348
PI3K Inhibitor	61103	1589	1133	1647	0.0233	0.0182	0.5090	0.0425	2722
Ribonucleotide Reductase Inhibitor	10429	1157	866	1172	0.1083	0.0767	0.5032	0.1496	2023
PKC Inhibitor	7323	2	38	2	0.0004	0.0052	0.5000	0.0054	40
EGFR Inhibitor	48472	90	641	77	0.0248	0.0131	0.4611	0.0146	731
Dihydrofolate Reductase Inhibitor	3442	290	615	227	0.0549	0.1516	0.4391	0.1841	905
Topoisomerase Inhibitor	19180	2952	2066	2030	0.0850	0.0972	0.4075	0.1562	5018
CDK Inhibitor	30761	1193	821	780	0.0257	0.0260	0.3953	0.0477	2014
Aurora Kinase Inhibitor	12960	25	458	16	0.0062	0.0341	0.3902	0.0352	483
NAMPT Inhibitor	8450	2070	798	1271	0.0756	0.0863	0.3804	0.1643	2868
HSP Inhibitor	21623	197	1060	118	0.0092	0.0467	0.3746	0.0512	1257
Niacinamide Phosphoribosyltransferase Inhibitor	1452	1884	476	1122	0.3576	0.2469	0.3733	0.3239	2360
Oxidative Stress Inducer	18	1890	8	1090	0.0162	0.3077	0.3658	0.3653	1898
RNA Polymerase Inhibitor	2362	2812	165	1570	0.0571	0.0653	0.3583	0.2511	2977
HDAC Inhibitor	48115	5854	1128	3209	0.0321	0.0229	0.3541	0.0744	6982
Microtubule Inhibitor	4491	1980	140	1057	0.0910	0.0302	0.3480	0.1561	2120
ATPase Inhibitor	12420	2761	757	1361	0.1466	0.0574	0.3302	0.1224	3518
Protein Synthesis Inhibitor	5975	536	870	255	0.0805	0.1271	0.3224	0.1473	1406
Tubulin Polymerization Inhibitor	6937	11972	985	5488	0.0938	0.1243	0.3143	0.2550	12957
PLK Inhibitor	11877	1519	1072	678	0.1384	0.0828	0.3086	0.1155	2591
Calcium Channel Blocker	71	2341	76	795	0.0717	0.5170	0.2535	0.2653	2417
PKC Activator	71	2341	76	795	0.0717	0.5170	0.2535	0.2653	2417
Survivin Inhibitor	24	4145	13	1396	0.0112	0.3514	0.2519	0.2526	4158
SRC Inhibitor	22086	254	593	77	0.0132	0.0261	0.2326	0.0291	847
Kinesin-Like Spindle Protein Inhibitor	299	562	26	165	0.1188	0.0800	0.2270	0.1815	588
Microtubule Stabilizing Agent	11	2956	4	663	0.0113	0.2667	0.1832	0.1835	2960
Cofilin Signaling Pathway Activator	3122	818	609	182	0.1179	0.1632	0.1820	0.1672	1427
Lim Kinase Activator	3122	818	609	182	0.1179	0.1632	0.1820	0.1672	1427
Rock Activator	3122	818	609	182	0.1179	0.1632	0.1820	0.1672	1427
Proteasome Inhibitor	8440	4901	314	1003	0.0904	0.0359	0.1699	0.0898	5215
NFKB Pathway Inhibitor	16753	4797	0	628	0.0001	0.0000	0.1158	0.0283	4797
P21 Activated Kinase Inhibitor	3552	86	91	8	0.0393	0.0250	0.0851	0.0265	177
BMX Inhibitor	4843	0	7	0	0.0000	0.0014		0.0014	7
DNA Dependent Protein Kinase Inhibitor	6478	0	19	0	0.0000	0.0029		0.0029	19
Farnesyltransferase Inhibitor	6941	0	19	0	0.0000	0.0027		0.0027	19
G Protein Coupled Receptor Agonist	1112	0	7	0	0.0000	0.0063		0.0063	7
Glycogen Synthase Kinase Inhibitor	11360	0	7	0	0.0000	0.0006		0.0006	7
HMGCR Inhibitor	11336	0	15	0	0.0000	0.0013		0.0013	15
HSP Antagonist	1284	0	78	0	0.0000	0.0573		0.0573	78
Hypoxia Inducible Factor Inhibitor	761	0	41	0	0.0000	0.0511		0.0511	41
Ion Channel Antagonist	3765	0	8	0	0.0000	0.0021		0.0021	8
Map Kinase Inhibitor	5954	0	29	0	0.0000	0.0048		0.0048	29
Phosphatidylinositol 3-Kinase (Pi3k) Inhibitor	2310	0	8	0	0.0000	0.0035		0.0035	8
Proteinase Activated Receptor Antagonist	5097	0	34	0	0.0000	0.0066		0.0066	34
RAD51 Inhibitor	1294	0	12	0	0.0000	0.0092		0.0092	12
Retinoid Receptor Ligand	554	0	7	0	0.0000	0.0125		0.0125	7
Ribosomal Protein Inhibitor	2444	0	7	0	0.0000	0.0029		0.0029	7

Sodium/Hydrogen Exchanger Inhibitor	1112	0	7	0	0.0000	0.0063		0.0063	7
TP53 Reactivator	4295	0	9	0	0.0000	0.0021		0.0021	9
Wee1 Kinase Inhibitor	4068	0	27	0	0.0000	0.0066		0.0066	27

Conclusion

This work performs a comprehensive study with 100 trials of 10-fold cross-validation analysis of anti-cancer drug response data. Two filtering techniques, based on AUC gap condition and the goodness of fitting dose response curve, were used to generate 10 different data subsets. The first part of this work identifies the data subset that gives the best model performance and investigates the effects of the filtering thresholds on the prediction performance. The highest MCC value of 0.635 is achieved in the analysis, which removes samples whose R-squared values resulted from dose response curve fitting are smaller than 0.9 and excludes samples with AUC values in the range of [0.4, 0.6] from the training set. This shows that applying data filtering approaches helps improve the model prediction performance. The second part of the work performs an in-depth analysis on the FPR, TPR and TFR of both cancer types and drug MoA categories, to identify the ones with high FPRs. The FPR of cancer type spans between 0.262 and 0.5189, while that of drug MoA category spans almost the full range of [0, 1]. Collecting more drug screening data for cancer types and drug MoA categories with high FPRs will potentially help developing more accurate prediction models. The post-prediction error analysis conducted in this study can be implemented as a pipeline module to be routinely applied after drug response prediction, which can conveniently provide a summary of prediction errors specific to cancer types and drug categories. This work can also be extended by performing such analysis with several drug response prediction models and conducting a comparison of their results.

Code availability

The source code of the deep neural network model is available at <https://github.com/ECP-CANDLE/Benchmarks/tree/master/Pilot1/Attn>

References

1. Zhu Y, Brettin T, Evrard YA, Partin A, Xia F, Shukla M, et al. Ensemble transfer learning for the prediction of anti-cancer drug response. *Sci Rep.* 2020;10.
2. Xia F, Shukla M, Brettin T, Garcia-Cardona C, Cohn J, Allen JE, et al. Predicting tumor cell line response to drug pairs with deep learning. *BMC Bioinformatics.* 2018;19.
3. Zhu Y, Brettin T, Xia F, Partin A, Shukla M, Yoo H, et al. Converting tabular data into images for deep learning with convolutional neural networks. *Sci Rep.* 2021;11.
4. Jin I, Nam H. HiDRA: Hierarchical Network for Drug Response Prediction with Attention. *Journal of Chemical Information and Modeling.* 2021;61:3858–67.
5. Manica M, Oskooei A, Born J, Subramanian V, Saéz-Rodríguez J, Rodríguez Martínez M. Toward Explainable Anticancer Compound Sensitivity Prediction via Multimodal Attention-Based Convolutional Encoders. *Mol Pharm.* 2019;:4797–806.
6. Zuo Z, Wang P, Chen X, Tian L, Ge H, Qian D. SWnet: a deep learning model for drug response prediction from cancer genomic signatures and compound chemical structures. *BMC Bioinformatics.* 2021;22.
7. Jiang Y, Rensi S, Wang S, Altman RB. DrugOrchestra: Jointly predicting drug response, targets, and side effects via deep multi-task learning. <https://doi.org/10.1101/2020.11.17.385757>.

8. Peres Da Silva R, Suphavitai C, Nagarajan N. TUGDA: Task uncertainty guided domain adaptation for robust generalization of cancer drug response prediction from in vitro to in vivo settings. *Bioinformatics*. 2021;37:176–83.
9. Li M, Wang Y, Zheng R, Shi X, Li Y, Wu FX, et al. DeepDSC: A Deep Learning Method to Predict Drug Sensitivity of Cancer Cell Lines. *IEEE/ACM Trans Comput Biol Bioinform*. 2021;18:575–82.
10. Tang Y-C, Gottlieb A. PathDSP: Explainable Drug Sensitivity Prediction through Cancer Pathway Enrichment Running title: Drug Sensitivity Prediction with Pathway. <https://doi.org/10.1101/2020.11.09.374132>.
11. Jiang L, Jiang C, Yu X, Fu R, Jin S, Liu X. DeepTTA: a transformer-based model for predicting cancer drug response. *Brief Bioinform*. 2022;23.
12. Rampásek L, Hidru D, Smirnov P, Haibe-Kains B, Goldenberg A. Dr.VAE: Improving drug response prediction via modeling of drug perturbation effects. *Bioinformatics*. 2019;35:3743–51.
13. Nguyen T, Nguyen GTT, Nguyen T, Le DH. Graph Convolutional Networks for Drug Response Prediction. *IEEE/ACM Trans Comput Biol Bioinform*. 2022;19:146–54.
14. Barretina J, Caponigro G, Stransky N, Venkatesan K, Margolin AA, Kim S, et al. The Cancer Cell Line Encyclopedia enables predictive modelling of anticancer drug sensitivity. *Nature*. 2012;483:603–7.
15. Haverty PM, Lin E, Tan J, Yu Y, Lam B, Lianoglou S, et al. Reproducible pharmacogenomic profiling of cancer cell line panels. *Nature*. 2016;533:333–7.
16. Yang W, Soares J, Greninger P, Edelman EJ, Lightfoot H, Forbes S, et al. Genomics of Drug Sensitivity in Cancer (GDSC): A resource for therapeutic biomarker discovery in cancer cells. *Nucleic Acids Res*. 2013;41.
17. Basu A, Bodycombe NE, Cheah JH, Price E V., Liu K, Schaefer GI, et al. An interactive resource to identify cancer genetic and lineage dependencies targeted by small molecules. *Cell*. 2013;154.
18. Shoemaker RH. The NCI60 human tumour cell line anticancer drug screen. *Nat Rev Cancer*. 2006;6:813–23.
19. Koletti A, Terryn R, Stathias V, Chung C, Cooper DJ, Turner JP, et al. Data Portal for the Library of Integrated Network-based Cellular Signatures (LINCS) program: Integrated access to diverse large-scale cellular perturbation response data. *Nucleic Acids Res*. 2018;46:D558–66.
20. Mauri A, Consonni V, Pavan M, Todeschini R. DRAGON software: An easy approach to molecular descriptor calculations. *Match*. 2006;56:237–48.
21. Wozniak JM, Jain R, Balaprakash P, Ozik J, Collier NT, Bauer J, et al. CANDLE/Supervisor: A workflow framework for machine learning applied to cancer research. *BMC Bioinformatics*. 2018;19.